Key Mediators of Somatic ATR Signaling Localize to Unpaired Chromosomes in Spermatocytes

Andrew M. Fedoriw[1], Debashish Menon[1], Yuna Kim[1], Weipeng Mu[1], and Terry Magnuson[1]

[1]Department of Genetics, Carolina Center for Genome Sciences, Lineberger Comprehensive Cancer Center, University of North Carolina at Chapel Hill, Chapel Hill, NC 27599

Keywords: Meiosis, Spermatogenesis, Transcriptional Regulation

Summary.

Meiotic silencing of unpaired chromatin (MSUC) occurs during the first meiotic prophase, as chromosomes that fail to pair are sequestered into a transcriptionally-repressive nuclear domain. This phenomenon is exemplified by the heterologous sex chromosomes of male mammals, where the ATR DNA damage response kinase is critical for this silencing event. However, the mechanisms underlying the initiation of MSUC remain unknown. Here, we show that essential components of ATR signaling in somatic cells are spatially confined to unpaired chromosomes in spermatocytes, including the ATR-dependent phosphorylation of the single-stranded DNA (ssDNA) binding complex, Replication Protein A (RPA) and the checkpoint kinase, CHK1. These observations support a model where ssDNA plays a central role in the recruitment of ATR during MSUC, and a link to meiotic progression, through activation of CHK1.

Introduction.

Transcription of protein-coding genes from the male sex chromosomes is repressed during the first meiotic prophase. This phenomenon is known as Meiotic Sex Chromosome Inactivation (MSCI), and is a consequence of the heterologous nature of the X and Y chromosomes. MSCI itself represents a specialized form of a mechanism not restricted to the sex chromosomes of males: any chromosome, or chromosomal region, that fails to pair (synapse) with a homolog will elicit an identical transcriptional response (known as Meiotic Silencing of Unsynapsed Chromatin, MSUC (Schimenti, 2005). Apart from a transcriptional response, activation of this pathway is closely linked with meiotic progression and may serve as a form of quality control, ensuring spermatocytes with excessive pairing defects are eliminated thereby preventing the formation of aneuploid gametes (Turner, 2007). However, it remains unclear how a meiotic chromosome can be distinguished on the basis of synapsis to elicit this distinctive transcriptional and physiological response.

Upon initiation of MSCI, the sex chromosomes undergo a pronounced cytological transformation, becoming sequestered into a specialized nuclear domain (known as the XY body) and depleted of elongating RNA polymerase II. Coincidently, the XY body becomes enriched for a significant number of factors involved in somatic DNA damage responses, many of which are distinct from those utilized in the repair of meiotic double stranded breaks (DSBs) by homologous recombination (HR). Ablation of the genes encoding the DNA damage proteins associated with the XY body phenotypically manifest as defective or incomplete MSCI and most often, meiotic arrest (Ichijima et al., 2012). Therefore, the DNA

repair machinery appears especially significant in activating this chromosome-wide form of transcriptional repression.

Among the proteins enriched on the XY body, the Ataxia Telangiectasia Mutated and RAD3 related (ATR) DNA damage response kinase plays a central role in MSCI activation (Royo et al., 2013). ATR is an early marker of MSCI: as homologous chromosomes undergo synapsis during the zygotene stage, ATR becomes enriched at unpaired (asynapsed) chromosomes and is responsible for catalyzing phosphorylation of the histone variant H2AFX near the axial elements (the proteinacious structure to which meiotic chromosomes are tethered). The spreading of H2AFX phosphorylation is dependent upon ATR and Mediator of DNA Damage Checkpoint 1 (MDC1), and is concomitant with the hallmark transcriptional silencing of MSCI (Fernandez-Capetillo et al., 2003; Ichijima et al., 2011; Royo et al., 2013). Despite its critical nature, the signal to which ATR is recruited during the early stages of MSCI remains undefined. Experimental evidence has suggested that initiation of MSCI is at least partially dependent on the BRCA1 protein (Turner et al., 2004; Broering et al., 2014). Together with ATR, localization of BRCA1 to asynapsed chromatin is an early event in meiosis. Deletion of exon 11 from the *Brca1* gene in the male germline compromises the activation of MSCI: ATR recruitment and H2AFX phosphorylation are reduced, but not entirely ablated, leading to MSCI failure. Despite this requirement, Broering *et al* have shown that other events in the early stages of MSCI, such as recruitment of the HORMAD proteins, is unaffected by the *Brca1* mutation (Broering et al., 2014). Therefore, additional, BRCA1-independent mechanisms are likely to participate in ATR activation during MSCI/MSUC.

In proliferating somatic cells, ATR is robustly activated by the presence of single-stranded DNA (ssDNA) bound by the heterotrimeric Replication Protein A (RPA) complex (Zou and Elledge, 2003). ssDNA/RPA can be generated through a number of mechanisms and DNA lesions, including the exonucleolytic processing of double-stranded breaks (DSBs) in preparation for HR, and stalled replication forks, when replicative DNA polymerases become uncoupled from associated DNA helicases. Once activated, ATR phosphorylates numerous targets to promote repair of the damaging lesion, and potentiates a response to control cell-cycle progression. Although unknown whether a similar mechanism elicits ATR activity during meiosis, ATR recruitment and MSUC can still occur in spermatocytes lacking the endonuclease responsible for generating meiotic DSBs, SPO11 (Bellani et al., 2005). Therefore, meiotic ATR activation appears not entirely dependent on the canonical mechanism for meiotic DSB formation. This has led to the proposal that SPO11-independent ssDNA regions underlie MSCI/MSUC initiation (Ichijima et al., 2012). In support of this hypothesis, foci of RPA and other repair proteins with affinity for ssDNA are detectable in spermatocytes with a catalytically-inactive *Spo11* mutant (Carofiglio et al., 2013), implying the presence of ssDNA generated independently of SPO11-dependent DSBs in the meiotic genome. If ATR recruitment to asynapsed chromatin is dependent upon ssDNA/RPA, these foci may represent genomic sites of meiotic ATR activation during the earliest phases of MSUC/MSCI.

To understand the mechanisms of MSCI initiation, we explored the hypothesis that if meiotic ATR activation were functionally related to well-studied mechanisms of ATR recruitment in somatic cells, then the hallmarks of somatic ATR activation should be enriched on the XY body. We focused on RPA itself,

since it can be phosphorylated in an ATR-dependent manner during replication stress (Anantha et al., 2007; Vassin et al., 2009; Shiotani et al., 2013). Phosphorylation of Serine 33 of the RPA32 (pRPA) subunit by ATR serves as a sensitive reporter of replication-induced DNA damage. Here, we demonstrate that the XY and asynapsed autosomes are highly enriched for pRPA. The presence of pRPA is dependent upon ATR, but independent of SPO11—consistent with known parameters of MSUC/MSCI initiation. Whereas RPA/ssDNA activates ATR, the checkpoint protein, CHK1, transduces ATR activation into physiological responses, including cell-cycle control and apoptosis (Liu et al., 2000). Coincident with the localization of pRPA and ATR, we demonstrate that asynapsed chromatin is similarly enriched for the active, phosphorylated forms of CHK1. Together, these data provide evidence for mechanistic similarities between MSUC and the DNA damage response to replication stress in somatic cells.

Results.

Phosphorylation of Serine 33 of RPA32 is a marker of asynapsis .

We first examined the distribution of phosphorylated RPA32-Serine 33 during the stages of the first meiotic prophase, relative to known markers of the XY body. MSCI/MSUC first initiates in late zygotene spermatocytes, as homologous chromosomes are completing synapsis. At this stage, ATR is recruited to asynapsed chromosomes and initiates H2AFX phosphorylation distinct from the ATM-dependent H2AFX phosphorylation of SPO11-dependent DSBs (add ref). When synapsis of homologous chromosomes is completed by the pachytene stage, the X and Y chromosomes are entirely coated with phosphorylated H2AFX (γH2AFX), and retain ATR. To determine whether pRPA is involved in MSCI, we used indirect immunofluorescence to examine the dynamics of pRPA in

primary spermatocytes. To identify specific stages within the first meiotic prophase, spermatocytes were co-stained with antibodies against γH2AFX and SCP3, a component of the axial element. pRPA accumulation was first clearly visible on a subset of axial elements in late zygotene spermatocytes, in which asynapsed chromosomes are first detected and marked by ATR-dependent H2AFX phosphorylation, and was coincident with BRCA1 (Fig.1A,B; Fig. S1,2). As meiosis progresses into the pachytene stage of the first meiotic prophase, formation of the XY body and associated transcriptional repression is complete. At this stage, pRPA was enriched on sex chromosomes of all pachytene spermatocytes, most intensely at the axial element (Fig. 1C,D). In agreement with these immunofluorescence observations, Western analysis of extracts from testes of postnatal mice showed a dramatic increase at day 10, coincident with the appearance of zygotene spermatocytes (Fig. S3)

To determine whether pRPA is a mark of the general MSUC pathway, we examined its localization in spermatocytes carrying an autosomal translocation between chromosomes 16 and 17 (Ts(16:17)65Dn (Epstein et al., 1985; Davisson et al., 1993)). The presence of these duplicated chromosomal regions will manifest as an asynapsed autosome in the XY body of spermatocytes, as one copy (either the translocation or its homologous regions on the native chromosomes) will fail to pair (Turner et al., 2005; Reinholdt et al., 2009). In 74% of pachytene spermatocytes from Ts(16:17)65Dn males, a second axial element complex was present within the γH2AFX domain, in addition to the X and Y chromosomes. In all of these spermatocytes, both the sex chromosomes and the asynapsed autosome were enriched for pRPA (Fig. 1E). Together, these data suggest the

phosphorylation of Serine 33 of RPA32 as a novel component of the MSUC pathway.

The axial element of the sex chromosomes is associated with numerous phosphoproteins, and axial element proteins of asyanpsed chromosomes are themselves highly phosphorylated (Fukuda et al., 2012). Although this pRPA antibody has been validated in other studies (Shiotani et al., 2013)., the high concentration of phosphoepitopes on the sex chromosomes may nonetheless contribute to non-specific binding. Therefore, we assessed the specificity of the pRPA antibody for immunofluorescence of spermatocyte spreads through competition with specific and nonspecific phosphopeptides. Pre-incubation of the pRPA antibody with its specific phosphopeptide reduced pRPA signal in pachytene spermatocytes, even at equal molar ratios between peptide and antibody (Fig. 2A,B, Fig.S4). To determine whether a nonspecific peptide could block the pRPA antibody, we utilized a phosphopeptide corresponding to a subunit of the cohesion complex, Structural Maintenance of Chromosomes 3 (SMC3). Serine 1083 (S1083) of SMC3 is a target of the ATR/ATM kinases, and this phosphorylated form of SMC3 (pSMC3) is enriched on the axial element of the meiotic sex chromosomes (Fukuda et al., 2012). Since S1083 is within a target motif for ATR phosphorylation, and the spatial enrichment of pSMC3 corresponds to where we observe the highest pRPA signal, we speculated that the presence of this epitope may contribute to nonspecific signal by the pRPA antibody. However, the pSMC3 peptide was unable to compete with the pRPA signal on the XY even at 1000X molar excess of peptide to antibody (Figure 2C).

ATR is required for the enrichment of pRPA on the meiotic sex chromosomes.

To confirm that the phosphorylation of RPA is related to ATR recruitment, we examined the distribution of pRPA in spermatocytes depleted of ATR. We utilized a strategy similar to Royo *et al*., inducing deletion of floxed *Atr* alleles by a tamoxifen-inducible CRE construct (Royo et al., 2013). As controls, age-matched $Atr^{fl/fl}$ males were treated with a similar course of tamoxifen. We recapitulated the published effects of ATR and γH2AFX distribution in spermatocytes from tamoxifen-treated $Atr^{fl/fl}$; *CAGG-CreERT2*/0 males (referred to as *Atr* cKO). In these spermatocytes, the remaining ATR is associated with the psuedoautosomal region of the sex chromosomes (Fig. 3A,B, arrows). Importantly, we found pRPA enrichment on the sex chromosomes of *Atr* cKO spermatocytes was diminished, and consistent with the lower levels and altered distribution of ATR (Fig. 3C,D). Immunostaining of spermatocytes from control and ATR *cKO* males with an antibody that detects RPA32 regardless of phosphorylation state revealed similar patterns of focal enrichment along the axial elements in both genotypes (Fig. 3E,F), suggesting the majority of the RPA32 signal is independent of ATR. Thus, the RPA associated with the meiotic sex chromosomes is subject to ATR-dependent phosphorylation.

RPA32 can also be phosphorylated by the Ataxia Telangiectasia Mutated (ATM) kinase, which is responsible for H2AFX phosphorylation in response to DSBs. Therefore, we examined the distribution of pRPA in $Atm^{-/-}$ spermatocytes. These mutant spermatocytes show significant pairing defects and arrest during early pachynema (Xu et al., 1996; Barlow et al., 1998; Barchi et al., 2005). However, pRPA remained associated with γH2AFX-coated axial elements in $Atm^{-/-}$

spermatocytes (Fig. S5A,B). These results confirm that ATR is the primary DNA damage kinase responsible for the phosphorylation of RPA32 on the XY body.

The accumulation and subsequent ATR-dependent phosphorylation of RPA at damaged replication forks in somatic cells is dependent on the MRN (MRE11-RAD50-NBS1) nuclease complex (Shiotani et al., 2013). The MRN complex catalyzes exonucleolytic processing of these lesions to produce long stretches of ssDNA/RPA. This accumulation of ssDNA/RPA recruits additional ATR, which in turn phosphorylates RPA. Interestingly, components of the MRN complex are known to associate with the XY, and in the case of NBS1, this association is independent of SPO11 (Barchi et al., 2005). However, the function of NBS1 and the MRN complex during MSCI has remained undefined. We speculated that the accumulation of pRPA on the XY body is linked to a similar processing mechanism, where ATR promotes MRN localization to the sex chromosomes to generate additional ssDNA/RPA. Thus, spermatocytes depleted for ATR should show a decrease MRN enrichment on the XY. We examined ATR-depleted spermatocytes for the distribution of NBS1, the MRN component with the most pronounced role in promoting pRPA accumulation in replicating somatic cells (Shiotani et al., 2013). In spermatocytes from wild-type animals, NBS1 was frequently associated with the XY, and we confirmed this association was SPO11-independent (Fig. 3G; Fig. S6). In contrast, NBS1 accumulation on the sex chromosomes was not observed in spermatocytes from *Atr* cKO males with undetectable levels of ATR (Fig. 3H). These data demonstrate that recruitment of NBS1 to the XY is not related to the processing of SPO11-dependent DSBs, but instead is elicited by ATR recruitment. However, the localization of NBS1 on the sex chromosomes is more diffuse than pRPA, suggesting the MRN complex may

have additional roles in MSCI, and perhaps underlie the foci of the ssDNA-binding protein RAD51 observed throughout the meiotic sex chromosomes (Plug et al., 1998). Together with the presence of pRPA, these observations suggest that the sex chromosomes may undergo a DNA-processing event as part of MSCI, linked to ATR recruitment.

pRPA is associated with asynapsed chromatin in the absence of SPO11-dependent meiotic DSBs.

SPO11 is an evolutionarily conserved enzyme responsible for generating the programmed double stranded breaks during meiosis. Because DSBs are required for successful synapsis, *Spo11*$^{-/-}$ spermatocytes are characterized by significant amounts of asynapsed chromosomes and fail to complete the first meiotic prophase (Baudat et al., 2000; Romanienko and Camerini-Otero, 2000). However, ATR enrichment and coincident transcriptional repression still occur, suggesting MSUC can be initiated in *Spo11*$^{-/-}$ spermatocytes (Mahadevaiah et al., 2008). Thus, if pRPA represents regions of meiotic ATR activation (rather than a processing event of DSBs on asynapsed chromosomes), then it should remain coincident with γH2AFX-coated chromosomes even in the absence of SPO11-dependent meiotic DSBs. In agreement with this prediction, 70% (n=189) of *Spo11*$^{-/-}$ spermatocytes with a single, clearly defined domain of γH2AFX had coincident enrichment of pRPA (Fig. 4A,B). In the remaining 30% of *Spo11*$^{-/-}$ spermatocytes, pRPA was present, yet more broadly distributed than γH2AFX (Fig. 4C). Therefore, these observations demonstrate that the phosphorylation of RPA occurs in *Spo11*$^{-/-}$ spermatocytes, and suggests that the ssDNA to which this RPA is bound is generated independently of the SPO11-dependent mechanism of DSB formation.

Phosphorylated CHK1 associates with asynapsed chromatin.

The accumulation of ssDNA/RPA during replication stress activates pathways to repair stalled replication forks, as well as a checkpoint pathway to elicit physiological responses such as control of the cell-cycle. This latter function is mediated through the ATR-dependent phosphorylation of CHK1, a checkpoint protein and potent physiological effector of ATR activity (Liu et al., 2000). Although CHK1 has previously been shown to associate with all axial elements in pachytene spermatocytes (Flaggs et al., 1997), we observed that CHK1 was highly enriched on the sex chromosomes (Fig. 5A). Furthermore, CHK1 phosphorylated at the ATR target residues serines 317 (S317) and 345 (S345), was detectable near the axial element of the sex chromosomes from late zygotene onwards (Fig. 5B,C; Fig. S7A,B). Consistent with these residues of CHK1 being direct targets of ATR kinase activity, phosphorylated CHK1 was not observed in spermatocytes depleted for ATR (Fig. 5D,E). In addition, pCHK1 accumulated on an asynapsed autosomal translocation and γH2AFX-coated axial elements of *Atm*$^{-/-}$ spermatocytes outside the XY body, demonstrating pCHK1 as a marker of asynapsed chromatin (Fig. S8). However, this pattern of enrichment was abrogated in *Spo11*$^{-/-}$ spermatocytes, despite pervasive asynapsis. Only 6% (n=47) and 22% (n=89) of mutant spermatocytes with a single, large domain of γH2AFX (identifying regions undergoing MSUC), had detectable colocalization of phosphorylated S317 and S345, respectively (Fig. 6A,B). Thus, in contrast to pRPA, the stable association of pCHK1 with asynasped chromosomes is strongly dependent on SPO11.

Discussion.

Activation of MSCI results in chromosome-wide transcriptional repression, a silent state that is maintained during the subsequent meiotic divisions (Turner, 2007). Although the ATR DNA damage response kinase plays an essential role in the initiation of this epigenetic phenomenon, the molecular signals that distinguish an asynapsed chromosome and recruit ATR to these genomic regions in primary spermatocytes have remained the subject of speculation. Recent observations of RPA foci in *Spo11*$^{-/-}$ spermatocytes, in which the MSUC pathway is still active, are indicative of ssDNA in meiotic genomes (Carofiglio et al., 2013). Given the critical role for RPA/ssDNA in stimulating ATR activation in somatic cells, it has been proposed that a similar mechanism may contribute to the recruitment and activation of ATR on asynapsed chromatin (Ichijima et al., 2012). Here, we demonstrate that asynapsed chromosomes are enriched for pRPA in an ATR dependent, but SPO11-independent manner. This enrichment is temporally coincident with MSCI activation, and the localization of pRPA near the axial elements of asynapsed chromosomes is spatially coincident with other factors involved in the early stages of MSCI. Since RPA is highly phosphorylated during ATR activation in somatic cells, marking genomic sites of DNA damage, we propose that regions of the sex chromosomes where pRPA accumulates would mark the DNA elements where the MSUC/MSCI response is initiated. These elements may act as sensors of pairing, becoming repaired or resolved into double-stranded DNA upon successful synapsis, while persisting as ssDNA where synapsis fails into late zygonema, when they serve as platforms for the activation of MSUC.

Like ATR, the DNA repair protein BRCA1 is an essential component of MSCI/MSUC activation, and one of the earliest cytological markers of asynapsed chromosomes. Although the best characterized role of BRCA1 in somatic DNA damage responses is promoting the repair of DSBs by HR, its function during MSCI/MSUC appears distinct from the recognition or repair of SPO11-dependent meiotic DSBs (Mahadevaiah et al., 2008; Broering et al., 2014). Therefore, how BRCA1 participates in the detection of asynasped chromatin to trigger ATR recruitment remains unknown. Interestingly, BRCA1 promotes ATR activation in response to UV-induced DNA damage in somatic cells (Pathania et al., 2011). UV irradiation results in the formation of bulky, covalent adducts to DNA, which impede or block the progression of replication forks. At UV-stalled replication forks, BRCA1 is required for the formation of long stretches of ssDNA which, when coated with RPA, will recruit and activate ATR. Thus, BRCA1 may serve a similar role during the early stages of MSCI/MSUC, increasing the size of SPO11-independent, RPA-coated ssDNA regions on asynapsed chromosomes to elicit high-levels of ATR activation. Notably, while ATR activation is severely affected in the majority of BRCA1-mutant spermatocytes, it is not entirely ablated, suggesting that some ssDNA/RPA regions are still present and may produce the limited ATR response observed in the absence of BRCA1.

It is not yet clear whether regions of SPO11-independent RPA may be a product of the DNA replication preceding meiotic entry, or a replication-independent process coordinated with the events of synapsis. Interestingly, a limited amount of replicative DNA synthesis has been reported to occur during zygonema, though the significance of this observation has remained enigmatic (Stern and Hotta, 1984; Hotta et al., 1985; Stubbs and Stern, 1986). In somatic cells, the most robust

phosphorylation of RPA occurs at replication-induced DSBs (Shiotani et al., 2013). These lesions are formed as the replication fork encounters a single-stranded break in the DNA strand, producing a 'single-ended' DSB. In this context, ATR promotes the recruitment of the MRN complex (including NBS1) to generate extensive ssDNA/RPA by resecting this DSB. Similarly, the ATR-dependent recruitment of NBS1 to the XY chromosomes suggest an ATR-dependent processing event is a component of MSCI. However, it is also possible that an ssDNA structure similar to that of a stalled replication fork may be generated independently of replicative DNA synthesis. For example, transcription may be a source of DNA damage (Sordet et al., 2009). Interestingly, the XY body is enriched for senataxin, a protein that functions in the resolution of RNA-DNA hybrids (R-loops) formed during transcriptional elongation (Becherel et al., 2013). If DNA lesions brought about by transcription were to play a role in the activation of the MSUC pathway, they would have to be formed in the early stages of the meiotic prophase since asynapsed regions are transcriptionally silenced. Regardless of their source, our observations provide support for a model where regions of ssDNA or ssDNA-bearing secondary structures are likely to play an important role in the activation of MSUC.

In addition to pRPA, we found the XY chromosomes enriched for active, phosphorylated forms of the checkpoint protein, CHK1, in an ATR-dependent manner. A previous report showed CHK1 broadly associated with the synaptonemal complexes of all chromosomes in mouse pachytene spermatocytes (Flaggs et al., 1997). The discrepancy with our observations may be related to the different antisera used. However, given the known dependence of CHK1 activation on ATR in somatic DNA damage pathways, and the enrichment of

ATR on the XY, we believe it is more likely that CHK1 is highly, if not exclusively, enriched on asynapsed chromosomes and a component of the MSUC pathway. Yet in contrast to the localization of pRPA, enrichment of pCHK1 to asynapsed chromosomes was severely compromised in *Spo11*$^{-/-}$ spermatocytes. Therefore, the physical association of CHK1 with asynapsed chromatin may be dependent upon SPO11-induced DSBs, or perhaps antagonized by the increased ATR activation brought about by excessive asynapsis in these mutant spermatocytes. Interestingly, shuttling of CHK1 into and out of the nucleus has been observed in somatic cells, and speculated as a mechanism by which CHK1 attenuates cell-cycle progression in response to DNA damage signaling (Smits et al., 2006; Wang et al., 2012). An analogous event may take place in *Spo11*$^{-/-}$ spermatocytes, where the extent of asynapsis crosses a critical threshold to elicit nuclear export of CHK1. Collectively, these data suggest CHK1 may function as a molecular link between ATR signaling at asynapsed chromosomes and meiotic progression, and reveal additional similarities between somatic ATR activation and MSCI/MSUC.

Materials and Methods.

Mouse Strains and Animal Work. *Atm*^{tm1Awb}, *Spo11*^{tm1Mjn}, Ts65(16:17)Dn, and B6.Cg-Tg(CAG-cre/Esr1)5Amc/J (*CAGG-CreERT2*) mice were obtained from Jackson Laboratories. Mice carrying a conditional allele of *Atr* have been previously described (Ruzankina et al., 2007). Genotyping for all alleles w was performed as previously described. To delete the floxed *Atr* allele, 5-8-week old *Atr*$^{fl/fl}$; *CAGG-CreERT2*/0 males were treated with 4mg of Tamoxifen (Sigma) for 2-4 doses at 48 hour intervals by intraperitoneal injection, and spermatocytes were harvested 10 days after the first treatment. All mouse work was performed in accordance with IACUC protocols at UNC.

Spermatocyte spreads. Spermatocyte spreads were made as described elsewhere(Peters et al., 1997), except slides were washed once for 5 minutes at room temperature in 0.32% Photoflo (Kodak)/1XPBS after fixing. Slides were air dried and stored at -80°C until use.

Immunoflouresence. Slides were washed for 10 minutes each at room temperature in 0.32% Photoflo/1X PBS, 0.1% Triton X100/1X PBS, and 0.3% BSA (Fisher)/1% donkey serum(Jackson ImmunoResearch)/0.015% Triton X-100/1XPBS. All primary antibodies were diluted in ADB buffer (3% BSA, 10% donkey serum, and 0.05% Triton X-100 in 1X PBS), and incubated overnight at 4°C, with the exception of RPA32 which was incubated for 1 hour at 37°C. After washing, slides were incubated for 1 hour at room temperature with secondary antibodies diluted in ADB buffer. Slides were then washed 3 times for 5 minutes each in 0.32% Photoflo/1X PBS. To detect γH2AFX, slides were then fixed for 10 minutes at room temperature with 4% paraformaldehyde (Electron Microscopy Sceinces)/1X PBS, washed extensively with 0.32% Photoflo/1X PBS, then incubated for 1-4 hours at room temperature with mouse-anti-γH2AFX (Millipore) directly labeled using the Alexa Fluor 488 Microscale Protein Labeling Kit according to manufacturer's instructions (Invitrogen), and diluted 1:200 in ADB. After 3, 5 minute

washes in 0.32% Photoflo/1X PBS, and one for 5 minutes with 0.32% Photoflo/ddH_2O, slides were mounted with SlowFade Gold (Invitrogen). Z-stacks of each channel were taken on a Ziess AxioImager M2 microscope, using the Axiovision software package (Zeiss). SCP3 and γH2AFX patterns were used to stage spermatocytes, and intensity adjusted for presentation purposes. Experiments were carried out in 2-3 animals per genotype and antibody. For peptide competition experiments, varying amounts of each peptide (Bethyl) were pre-incubated with the antibody for 30 minutes at room temperature in ADB buffer prior to immunofluorescence.

Antibodies. The following primary antibodies (and dilutions) were used for immunoflouresence: rabbit-anti-phosphoRPA32, Serine 33 (Bethyl, 1:200); rabbit-anti-RPA32 (Bethyl, 1:100); SCP3 (Abcam, 1:500), mouse-anti-BRCA1 (a gift from David Livingston, 1:50); rabbit-anti-phosphoCHK1, Serine 317 (Cell Signaling, 1:25); rabbit-anti-phosphoCHK1, Serine 345 (Cell Signaling, 1:50); rabbit-anti-ATR (Calbiochem 1:400), mouse-anti-NBS1 (BD Biosciences, 1:10). Secondary antibodies, goat-anti-rabbit-Alexa647, goat-anti-mouse-Alexa568, goat-anti-rabbit-Alexa568, or goat-anti-mouse-Alexa488 (Invitrogen) were diluted 1:500. DNA was counterstained with DAPI. Phospho-specific antibodies did not produce a signal when tested against phosphatase-treated spermatocyte spreads.

Acknowledgements.

We thank Drs. Cyrus Vaziri, Joshua Starmer, and members of the Magnuson Laboratory for critical reading of the manuscript.

Funding.

This work was supported by 1F32HD052413 to A.M.F, R01-GM10974 and DPU-U01-14817 to T.R.M.

Competing Financial Interests.

The authors declare no competing financial interests.

Author Contributions.

A.M.F. conceived, designed, and performed the experiments with input from T.M. D.M., Y.K., and W.M. performed the experiments. A.M.F. and T.M. prepared the manuscript. All authors commented on the manuscript.

References.

Anantha, R. W., Vassin, V. M. and Borowiec, J. A. (2007). Sequential and synergistic modification of human RPA stimulates chromosomal DNA repair. *The Journal of biological chemistry* **282**, 35910-35923.

Barchi, M., Mahadevaiah, S., Di Giacomo, M., Baudat, F., de Rooij, D. G., Burgoyne, P. S., Jasin, M. and Keeney, S. (2005). Surveillance of different recombination defects in mouse spermatocytes yields distinct responses despite elimination at an identical developmental stage. *Molecular and cellular biology* **25**, 7203-7215.

Barlow, C., Liyanage, M., Moens, P. B., Tarsounas, M., Nagashima, K., Brown, K., Rottinghaus, S., Jackson, S. P., Tagle, D., Ried, T. et al. (1998). Atm deficiency results in severe meiotic disruption as early as leptonema of prophase I. *Development* **125**, 4007-4017.

Baudat, F., Manova, K., Yuen, J. P., Jasin, M. and Keeney, S. (2000). Chromosome synapsis defects and sexually dimorphic meiotic progression in mice lacking Spo11. *Mol Cell* **6**, 989-998.

Becherel, O. J., Yeo, A. J., Stellati, A., Heng, E. Y., Luff, J., Suraweera, A. M., Woods, R., Fleming, J., Carrie, D., McKinney, K. et al. (2013). Senataxin plays an essential role with DNA damage response proteins in meiotic recombination and gene silencing. *PLoS Genet* **9**, e1003435.

Bellani, M. A., Romanienko, P. J., Cairatti, D. A. and Camerini-Otero, R. D. (2005). SPO11 is required for sex-body formation, and Spo11 heterozygosity rescues the prophase arrest of Atm-/- spermatocytes. *Journal of cell science* **118**, 3233-3245.

Broering, T. J., Alavattam, K. G., Sadreyev, R. I., Ichijima, Y., Kato, Y., Hasegawa, K., Camerini-Otero, R. D., Lee, J. T., Andreassen, P. R. and Namekawa, S. H.

(2014). BRCA1 establishes DNA damage signaling and pericentric heterochromatin of the X chromosome in male meiosis. *J Cell Biol* **205**, 663-675.

Carofiglio, F., Inagaki, A., de Vries, S., Wassenaar, E., Schoenmakers, S., Vermeulen, C., van Cappellen, W. A., Sleddens-Linkels, E., Grootegoed, J. A., Te Riele, H. P. et al. (2013). SPO11-independent DNA repair foci and their role in meiotic silencing. *PLoS genetics* **9**, e1003538.

Davisson, M. T., Schmidt, C., Reeves, R. H., Irving, N. G., Akeson, E. C., Harris, B. S. and Bronson, R. T. (1993). Segmental trisomy as a mouse model for Down syndrome. *Progress in clinical and biological research* **384**, 117-133.

Epstein, C. J., Cox, D. R. and Epstein, L. B. (1985). Mouse trisomy 16: an animal model of human trisomy 21 (Down syndrome). *Annals of the New York Academy of Sciences* **450**, 157-168.

Fernandez-Capetillo, O., Mahadevaiah, S. K., Celeste, A., Romanienko, P. J., Camerini-Otero, R. D., Bonner, W. M., Manova, K., Burgoyne, P. and Nussenzweig, A. (2003). H2AX is required for chromatin remodeling and inactivation of sex chromosomes in male mouse meiosis. *Dev Cell* **4**, 497-508.

Flaggs, G., Plug, A. W., Dunks, K. M., Mundt, K. E., Ford, J. C., Quiggle, M. R., Taylor, E. M., Westphal, C. H., Ashley, T., Hoekstra, M. F. et al. (1997). Atm-dependent interactions of a mammalian chk1 homolog with meiotic chromosomes. *Curr Biol* **7**, 977-986.

Fukuda, T., Pratto, F., Schimenti, J. C., Turner, J. M., Camerini-Otero, R. D. and Hoog, C. (2012). Phosphorylation of chromosome core components may serve as axis marks for the status of chromosomal events during mammalian meiosis. *PLoS Genet* **8**, e1002485.

Hotta, Y., Tabata, S., Stubbs, L. and Stern, H. (1985). Meiosis-specific transcripts of a DNA component replicated during chromosome pairing: homology across the phylogenetic spectrum. *Cell* **40**, 785-793.

Ichijima, Y., Sin, H. S. and Namekawa, S. H. (2012). Sex chromosome inactivation in germ cells: emerging roles of DNA damage response pathways. *Cellular and molecular life sciences : CMLS* **69**, 2559-2572.

Ichijima, Y., Ichijima, M., Lou, Z., Nussenzweig, A., Camerini-Otero, R. D., Chen, J., Andreassen, P. R. and Namekawa, S. H. (2011). MDC1 directs chromosome-wide silencing of the sex chromosomes in male germ cells. *Genes Dev* **25**, 959-971.

Liu, Q., Guntuku, S., Cui, X. S., Matsuoka, S., Cortez, D., Tamai, K., Luo, G., Carattini-Rivera, S., DeMayo, F., Bradley, A. et al. (2000). Chk1 is an essential kinase that is regulated by Atr and required for the G(2)/M DNA damage checkpoint. *Gene Dev* **14**, 1448-1459.

Mahadevaiah, S. K., Bourc'his, D., de Rooij, D. G., Bestor, T. H., Turner, J. M. and Burgoyne, P. S. (2008). Extensive meiotic asynapsis in mice antagonises meiotic silencing of unsynapsed chromatin and consequently disrupts meiotic sex chromosome inactivation. *The Journal of cell biology* **182**, 263-276.

Pathania, S., Nguyen, J., Hill, S. J., Scully, R., Adelmant, G. O., Marto, J. A., Feunteun, J. and Livingston, D. M. (2011). BRCA1 Is Required for Postreplication Repair after UV-Induced DNA Damage. *Molecular Cell*, 235-251.

Peters, A. H., Plug, A. W., van Vugt, M. J. and de Boer, P. (1997). A drying-down technique for the spreading of mammalian meiocytes from the male and female germline. *Chromosome Res* **5**, 66-68.

Plug, A. W., Peters, A. H., Keegan, K. S., Hoekstra, M. F. and de Boer, P. (1998). Changes in protein composition of meiotic nodules during mammalian meiosis. *J Cell Sci* **111**, 412-423.

Reinholdt, L. G., Czechanski, A., Kamdar, S., King, B. L., Sun, F. and Handel, M. A. (2009). Meiotic behavior of aneuploid chromatin in mouse models of Down syndrome. *Chromosoma* **118**, 723-736.

Romanienko, P. J. and Camerini-Otero, R. D. (2000). The mouse Spo11 gene is required for meiotic chromosome synapsis. *Mol Cell* **6**, 975-987.

Royo, H., Prosser, H., Ruzankina, Y., Mahadevaiah, S. K., Cloutier, J. M., Baumann, M., Fukuda, T., Hoog, C., Toth, A., de Rooij, D. G. et al. (2013). ATR acts stage specifically to regulate multiple aspects of mammalian meiotic silencing. *Gene Dev* **27**, 1484-1494.

Ruzankina, Y., Pinzon-Guzman, C., Asare, A., Ong, T., Pontano, L., Cotsarelis, G., Zediak, V. P., Velez, M., Bhandoola, A. and Brown, E. J. (2007). Deletion of the developmentally essential gene ATR in adult mice leads to age-related phenotypes and stem cell loss. *Cell Stem Cell* **1**, 113-126.

Schimenti, J. (2005). Synapsis or silence. *Nat Genet* **37**, 11-13.

Shiotani, B., Nguyen, H. D., Hakansson, P., Marechal, A., Tse, A., Tahara, H. and Zou, L. (2013). Two distinct modes of ATR activation orchestrated by Rad17 and Nbs1. *Cell Rep* **3**, 1651-1662.

Smits, V. A., Reaper, P. M. and Jackson, S. P. (2006). Rapid PIKK-dependent release of Chk1 from chromatin promotes the DNA-damage checkpoint response. *Current biology : CB* **16**, 150-159.

Sordet, O., Redon, C. E., Guirouilh-Barbat, J., Smith, S., Solier, S., Douarre, C., Conti, C., Nakamura, A. J., Das, B. B., Nicolas, E. et al. (2009). Ataxia telangiectasia

mutated activation by transcription- and topoisomerase I-induced DNA double-strand breaks. *EMBO Rep* **10**, 887-893.

Stern, H. and Hotta, Y. (1984). Chromosome organization in the regulation of meiotic prophase. *Symposia of the Society for Experimental Biology* **38**, 161-175.

Stubbs, L. and Stern, H. (1986). DNA synthesis at selective sites during pachytene in mouse spermatocytes. *Chromosoma* **93**, 529-536.

Turner, J. M. (2007). Meiotic sex chromosome inactivation. *Development* **134**, 1823-1831.

Turner, J. M., Mahadevaiah, S. K., Fernandez-Capetillo, O., Nussenzweig, A., Xu, X., Deng, C. X. and Burgoyne, P. S. (2005). Silencing of unsynapsed meiotic chromosomes in the mouse. *Nature genetics* **37**, 41-47.

Turner, J. M., Aprelikova, O., Xu, X., Wang, R., Kim, S., Chandramouli, G. V., Barrett, J. C., Burgoyne, P. S. and Deng, C. X. (2004). BRCA1, histone H2AX phosphorylation, and male meiotic sex chromosome inactivation. *Curr Biol* **14**, 2135-2142.

Vassin, V. M., Anantha, R. W., Sokolova, E., Kanner, S. and Borowiec, J. A. (2009). Human RPA phosphorylation by ATR stimulates DNA synthesis and prevents ssDNA accumulation during DNA-replication stress. *Journal of cell science* **122**, 4070-4080.

Wang, J., Han, X., Feng, X., Wang, Z. and Zhang, Y. (2012). Coupling cellular localization and function of checkpoint kinase 1 (Chk1) in checkpoints and cell viability. *J Biol Chem* **287**, 25501-25509.

Xu, Y., Ashley, T., Brainerd, E. E., Bronson, R. T., Meyn, M. S. and Baltimore, D. (1996). Targeted disruption of ATM leads to growth retardation, chromosomal fragmentation during meiosis, immune defects, and thymic lymphoma. *Gene Dev* **10**, 2411-2422.

Zou, L. and Elledge, S. J. (2003). Sensing DNA damage through ATRIP recognition of RPA-ssDNA complexes. *Science* **300**, 1542-1548.

Figures

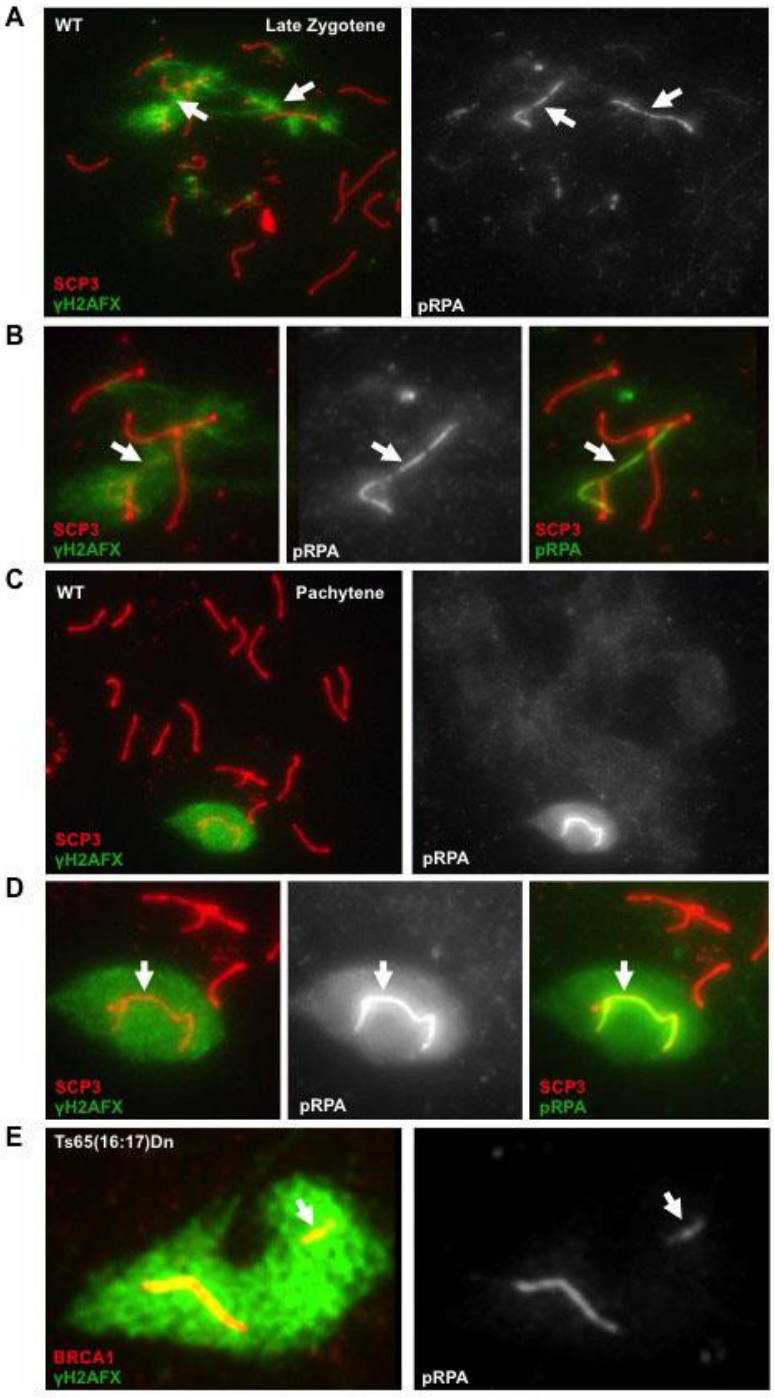

Fig. 1. Phosphorylated RPA is a mark of asynapsed chromosomes in primary spermatocytes. (**A**) RPA32 phosphorylated at Serine 33 (pRPA) first colocalizes with the γH2AFX -coated sex chromosomes of wild-type (WT) late zygotene spermatocytes (white arrows). Higher magnification of dotted box is shown in (**B**). (**C**) The sex

chromosomes of all pachytene spermatocytes are enriched for pRPA. (**D**) Higher magnification view of XY body from (**C**). For (**B**) and (**D**), pRPA staining is highest near axial element (arrow) (**E**) An unpaired autosome in the XY body of Ts65(16:17)Dn spermatocytes, marked by BRCA1 and γH2AFX, is also enriched for pRPA. The arrowhead indicates the autosomal translocation**.**

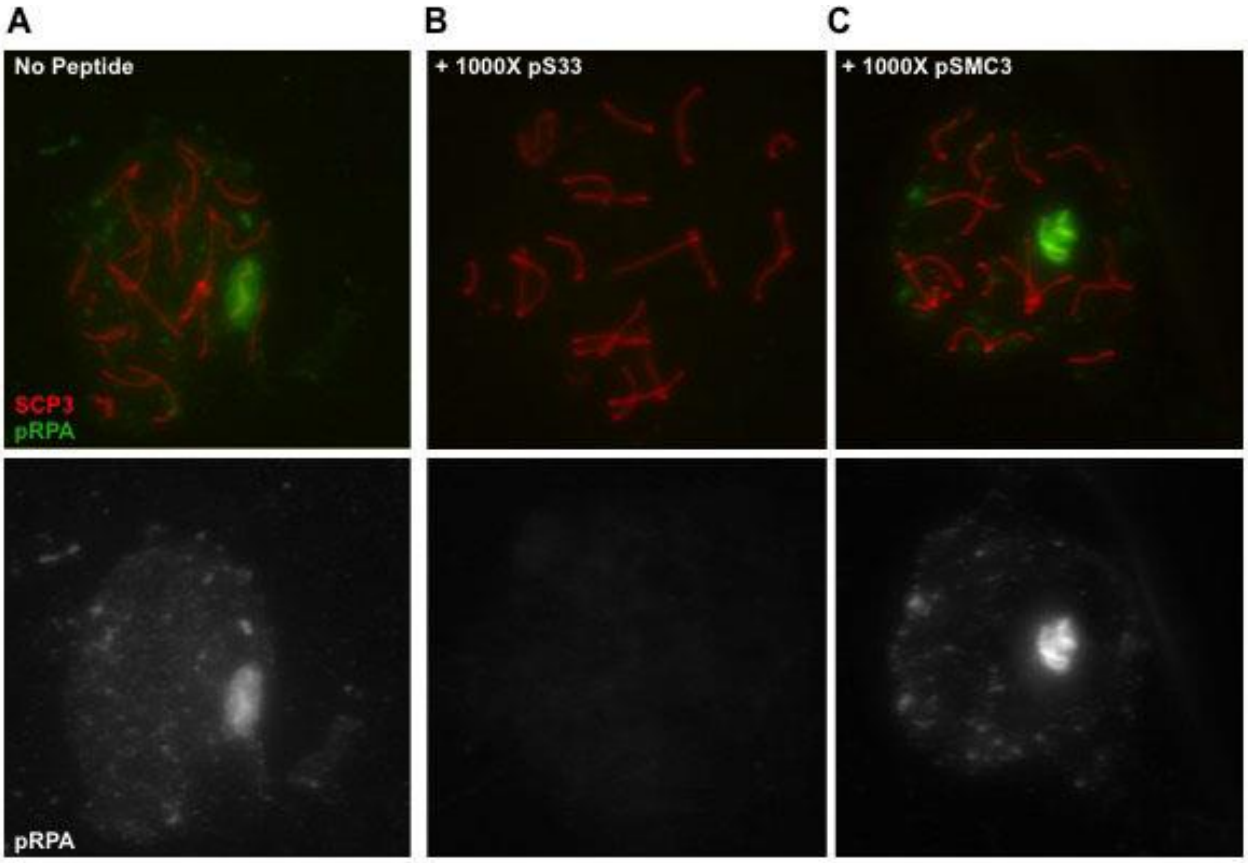

Fig. 2. Specificity of pRPA antibody. WT spermatocytes were incubated with a molar excess of specific or non-specific phosphopeptides, along with antibodies against pRPA. The pRPA signal associated with the XY (**A**) was completely abolished in the presence of a peptide specific for this antibody (pS33) (**B**). In contrast, even a 1000-fold molar excess of a peptide corresponding to SMC3, a known component of the XY body, had no effect on the association of the pRPA antibody with the sex chromosomes (**C**).

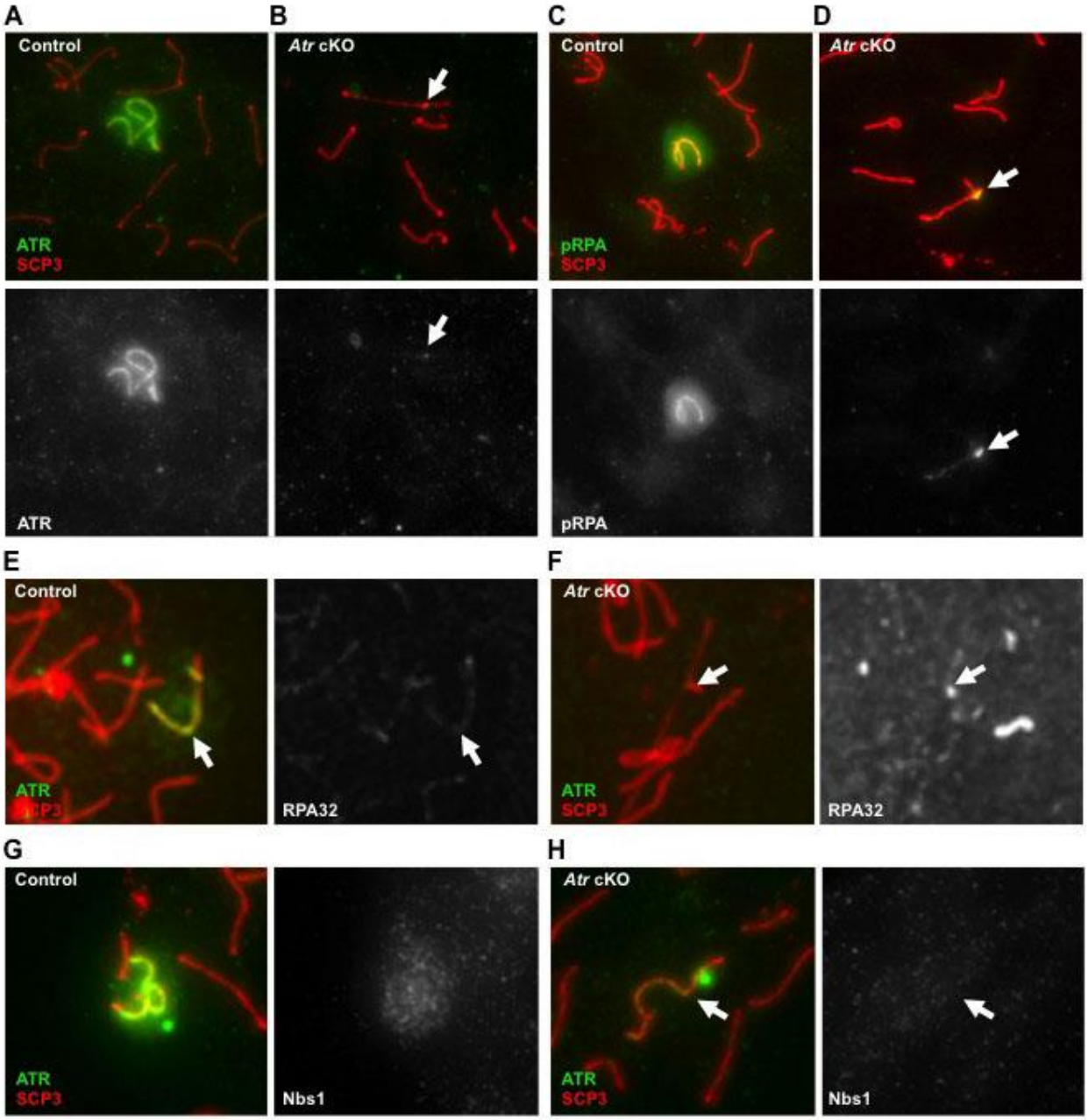

Fig. 3. The phosphorylation of RPA on the meiotic sex chromosomes is dependent on ATR. ATR protein levels in spermatocytes from control (**A**) and *Atr* cKO (**B**) males. pRPA enrichment on the XY in control (**C**) and *Atr* cKO (**D**) spermatocytes. Immunostaining with antibodies against RPA32, a component of the RPA complex, show similar focal patterns in control pachytene spermatocytes (**E**) and spermatocytes from *Atr*

cKO males with undetectable ATR protein (**F**). In control spermatocytes, the NBS1 nuclease is associated with the XY body. In contrast, *Atr* cKO spermatocytes with low levels of ATR (**H**) had undetectable Nbs1 enrichment on these chromosomes. In (**B**) and (**D**) through (**H**), white arrow designates the sex chromosomes.

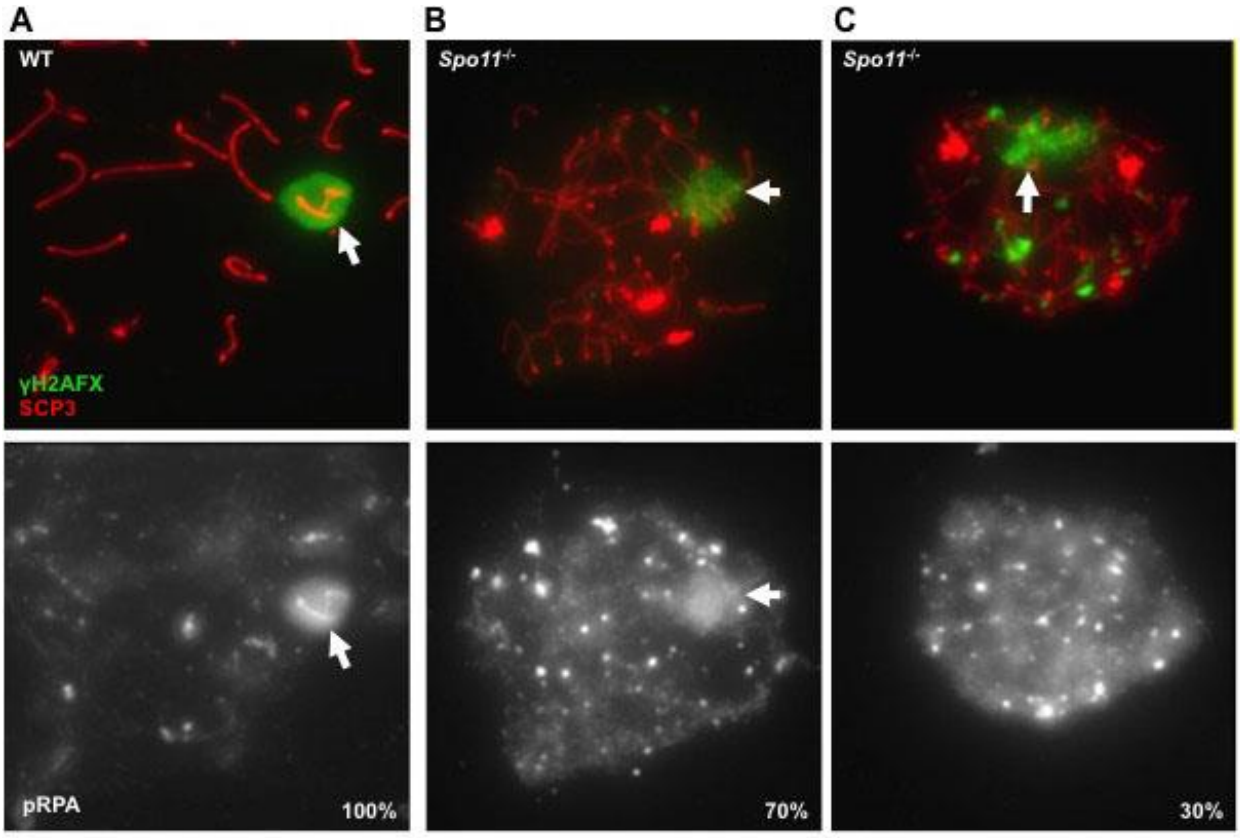

Fig. 4. Phosphorylation of RPA is independent of *Spo11*. (**A**) pRPA is associated with the XY chromosomes in 100% of WT spermatocytes. (**B**) 70% of *Spo11*$^{-/-}$ spermatocytes show colocalization of pRPA with γH2AFX-positive domains. (**C**) Broad, nuclear pRPA distribution is evident in 30% of mutant spermatocytes. Bright pRPA foci are common in both classes of *Spo11*$^{-/-}$ spermatocytes.

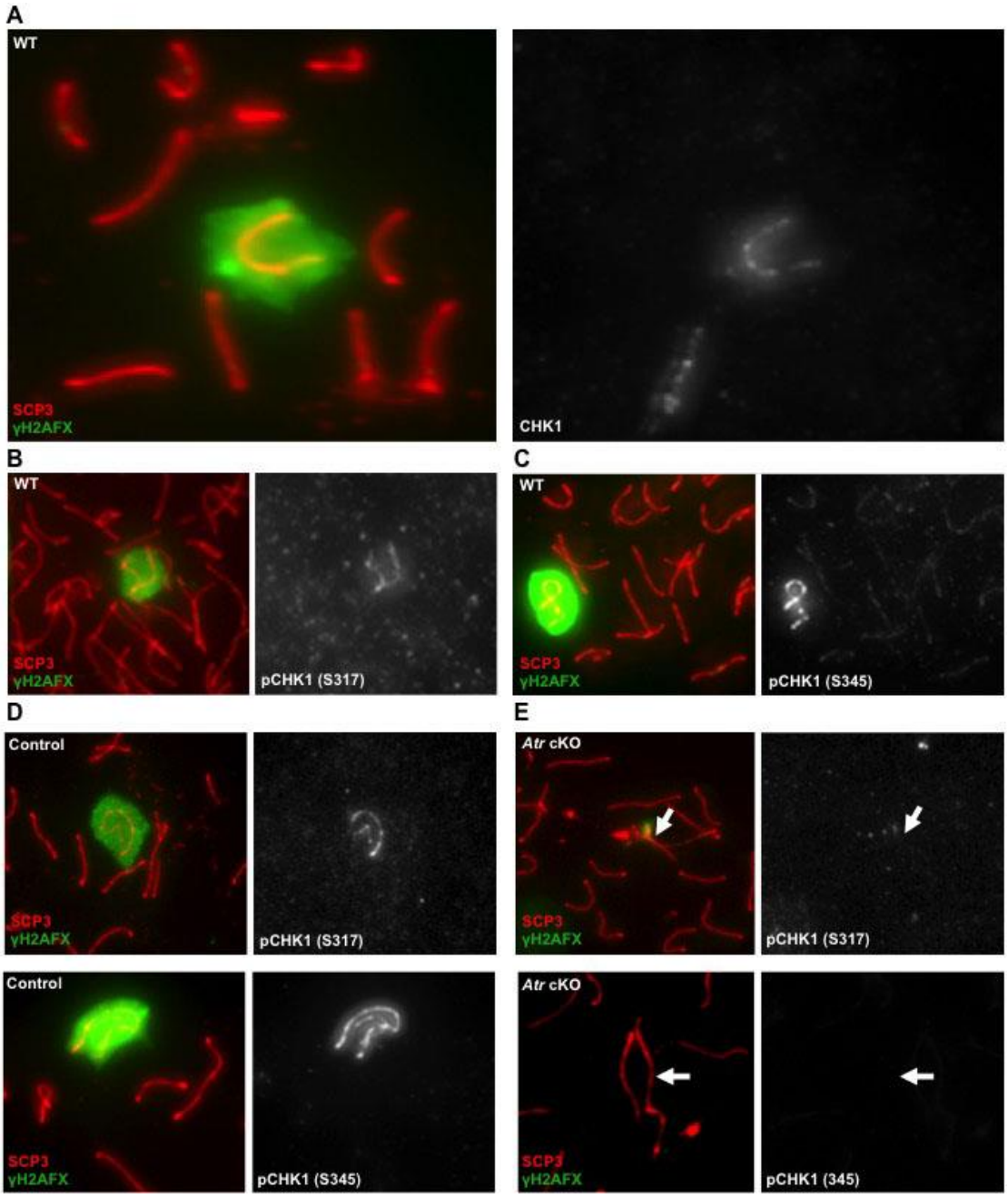

Fig. 5. ATR-dependent localization and phosphorylation of CHK1 on the XY body. The asynapsed sex chromosomes show enrichment of the checkpoint protein, CHK1 in WT spermatocytes (**A**). Furthermore, the XY body of WT spermatocytes is associated with phosphorylated forms of CHK1: Serine 317 (S317) (**B**) and Serine 345 (S345) (**C**), both target residues of the ATR kinase. The enrichment of pCHK1, S317 and S345,is

undetectable in spermatocytes from *Atr* cKO males (**D**) and (**E**) respectively; white arrows indicate the position of the XY chromosomes.

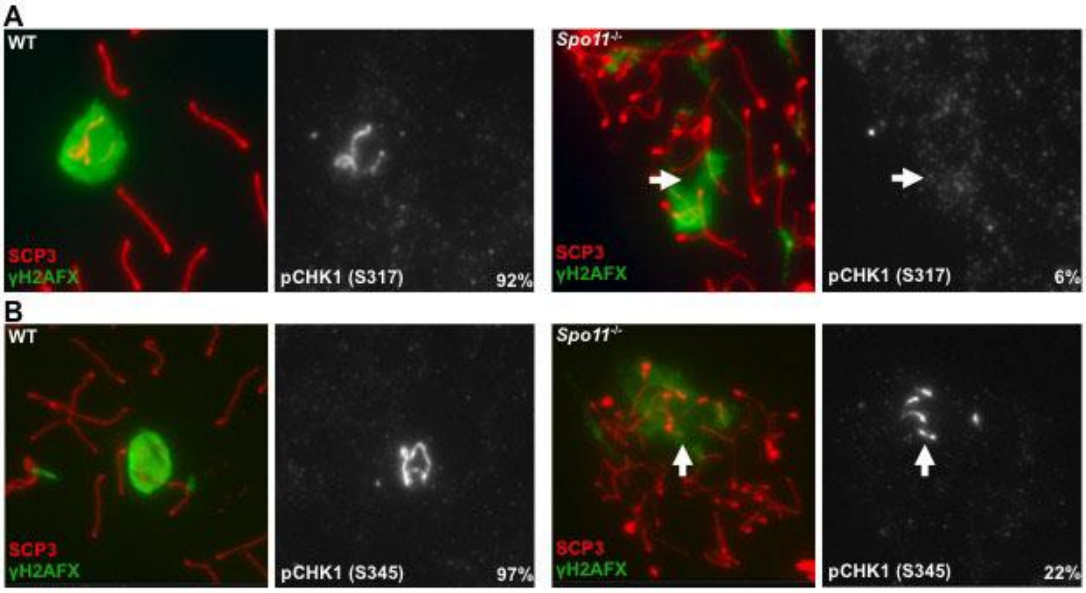

Fig. 6. *Spo11*-deficiency severely abrogates the association of pCHK1 with asynapsed chromatin. Localization of pCHK1 (S317) (**A**), and pCHK1 (S345) (**B**) to the sex chromosomes and regions undergoing MSUC in WT and *Spo11*$^{-/-}$ spermatocytes, respectively.

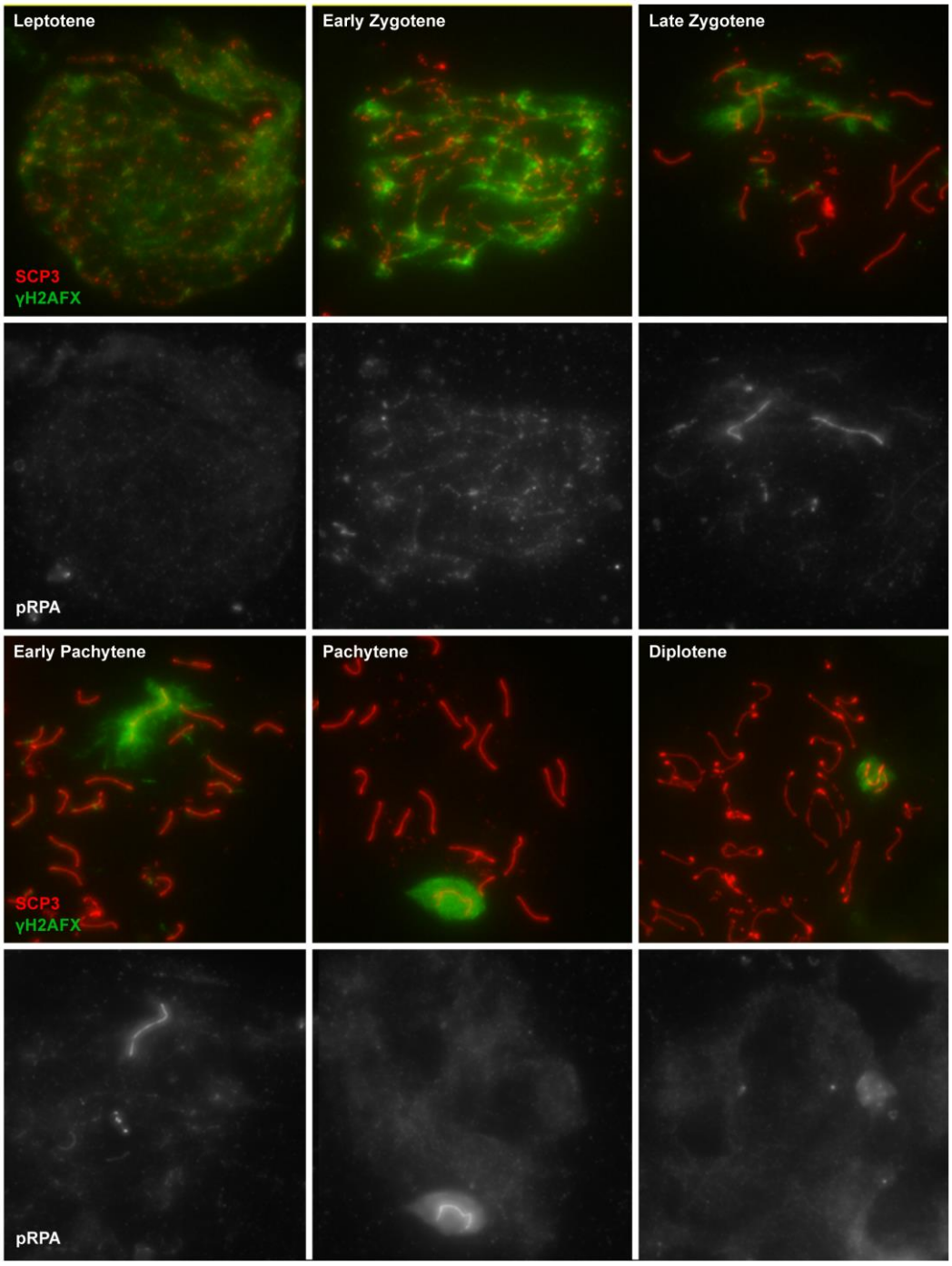

Fig. S1. Dynamics of pRPA during the first meiotic prophase. Immunofluoresence of pRPA, γH2AFX, and a component of the axial element, SCP3, in WT spermatocytes at individual stages of the first meiotic prophase. Representative immunofluorescence images from WT males.

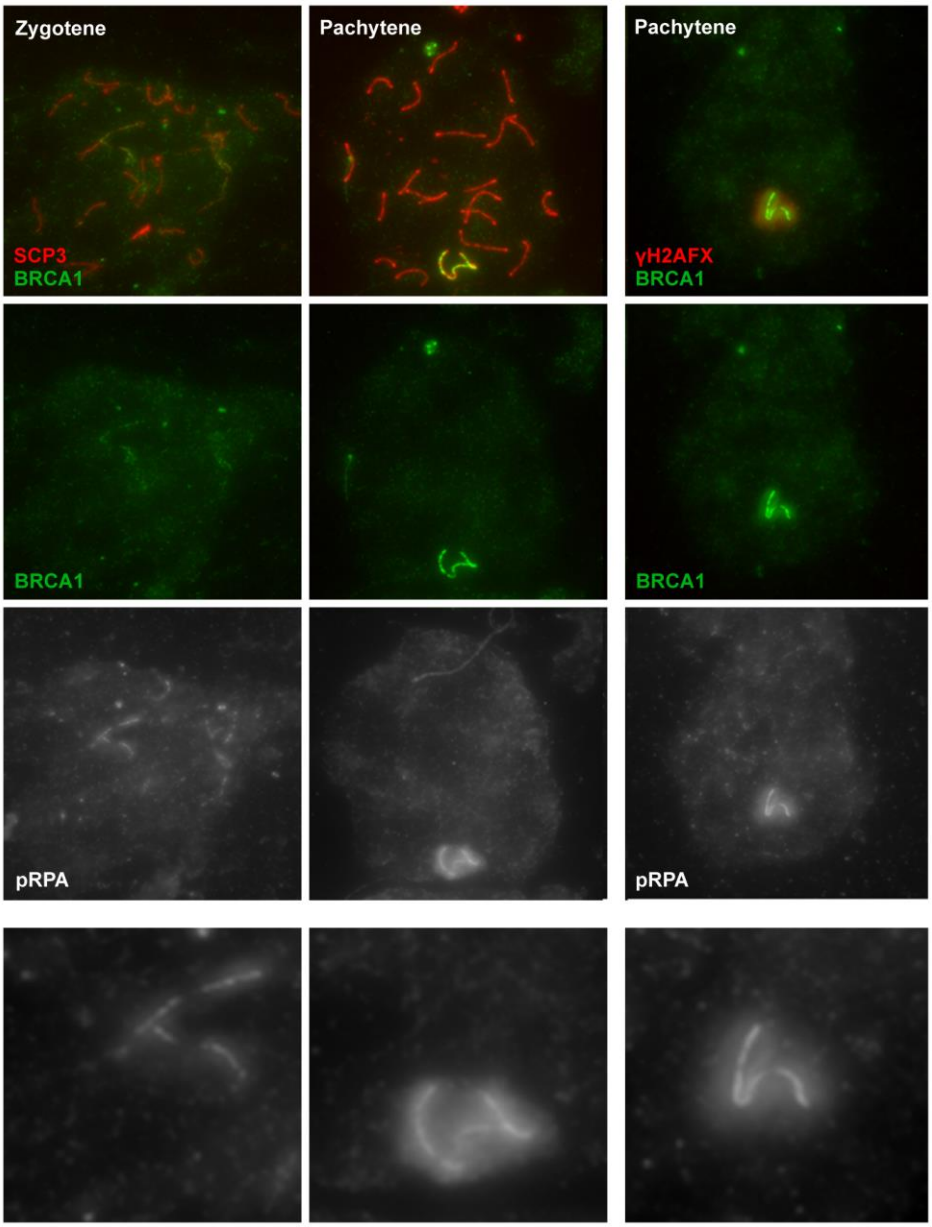

Fig. S2. pRPA enrichment is coincident with BRCA1 staining on the XY.

(**A**) pRPA in WT zygotene and pachytene spermatocytes colocalizes with BRCA1, a marker of asynapsed chromosomes. Note, pRPA staining pattern is similar regardless of co-staining with antibodies against BRCA1 or γH2AFX, suggesting signal is not a result of 'bleed through' of BRCA1 or γH2AFX immunoflourescent signal. (**B**) Higher maginification view of XY body from spermatocytes in (**A**).

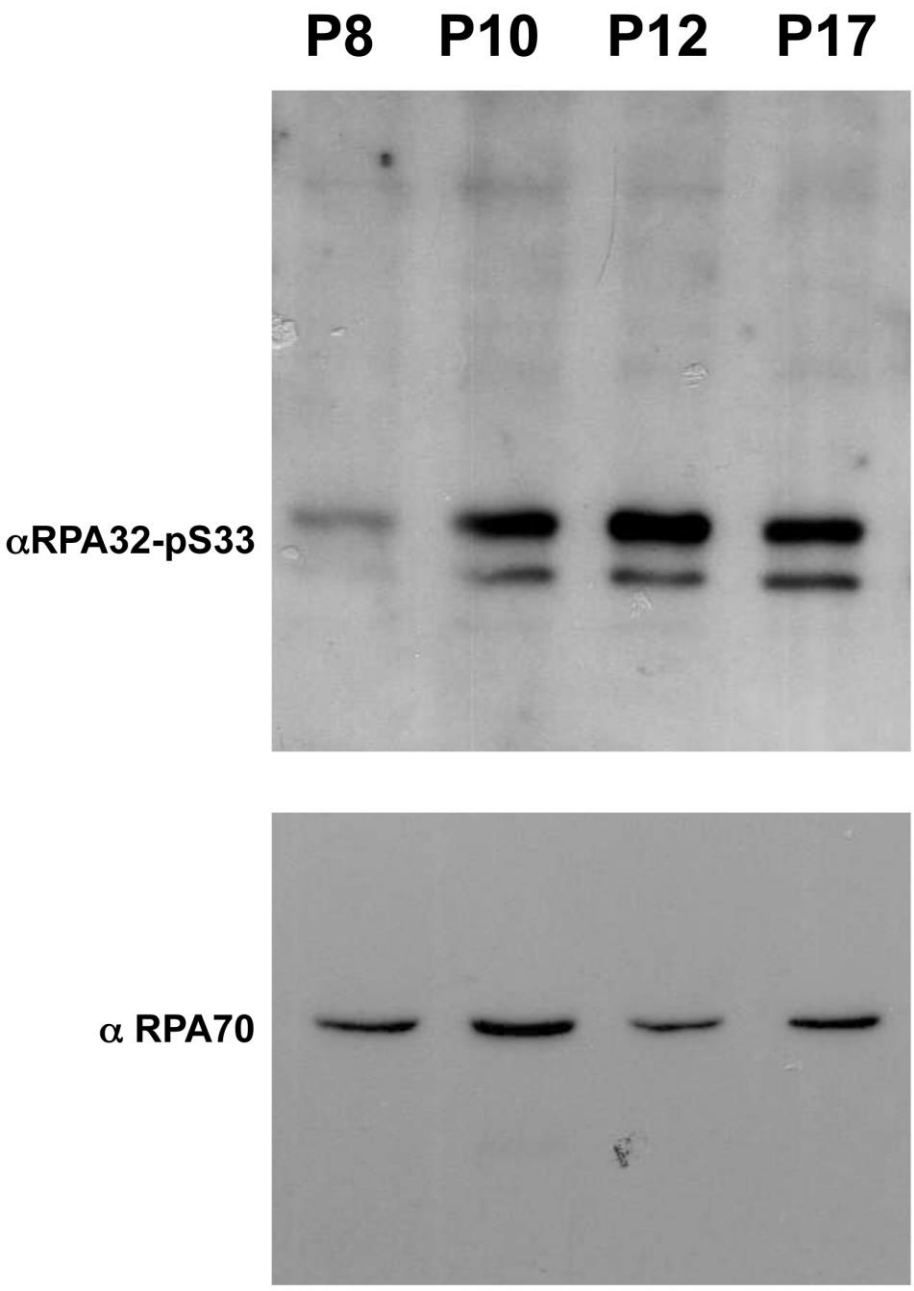

Fig. S3. Levels of phosphorylated RPA in postnatal testes. Levels of pRPA and RPA70 were assessed in whole cell extracts from testes of postnatal days 8 (P8), 10 (P10), 12 (P12), and 17 (P17). At P10, leptotene and zygotene spermatocytes are first evident.

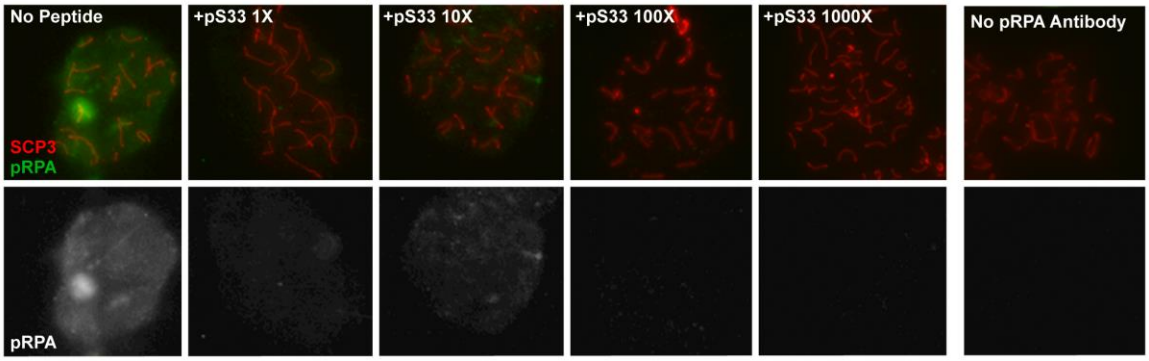

Fig. S4. Specificity of the anti-pRPA antibody determined by peptide competition. Anti-pRPA antibodies were pre-incubated with varying amounts of the immunizing peptide, ranging from an equal-molar ratio to a 1000-fold excess, then used for immunofluorescence experiments on control spermatocytes. Signal on the XY was diminished at an equal-molar excess.

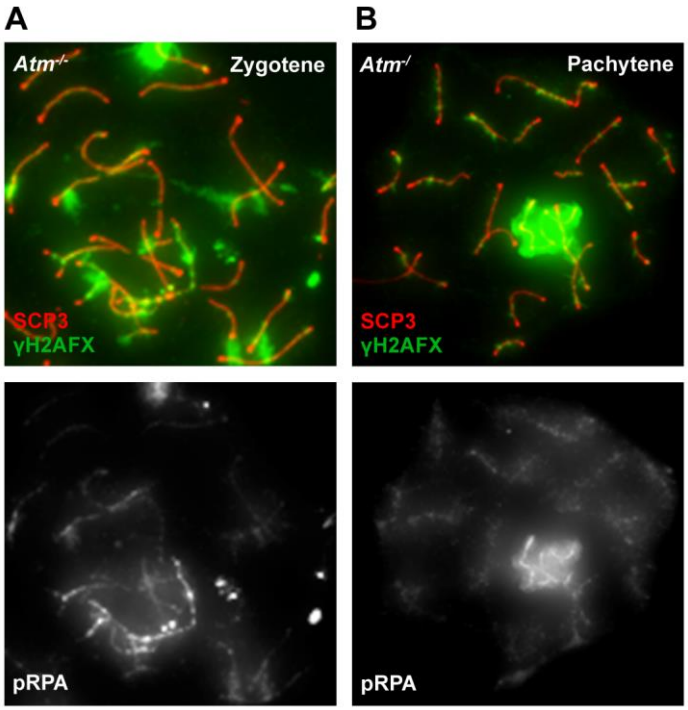

Fig. S5. RPA phosphorylation is unaffected in the absence of the ATM kinase. Zygotene (**A**) and more developmentally advanced, pachytene-like (**B**) *Atm*$^{-/-}$ spermatocytes show normal patterns of colocalization between pRPA and γH2AFX-positive domains.

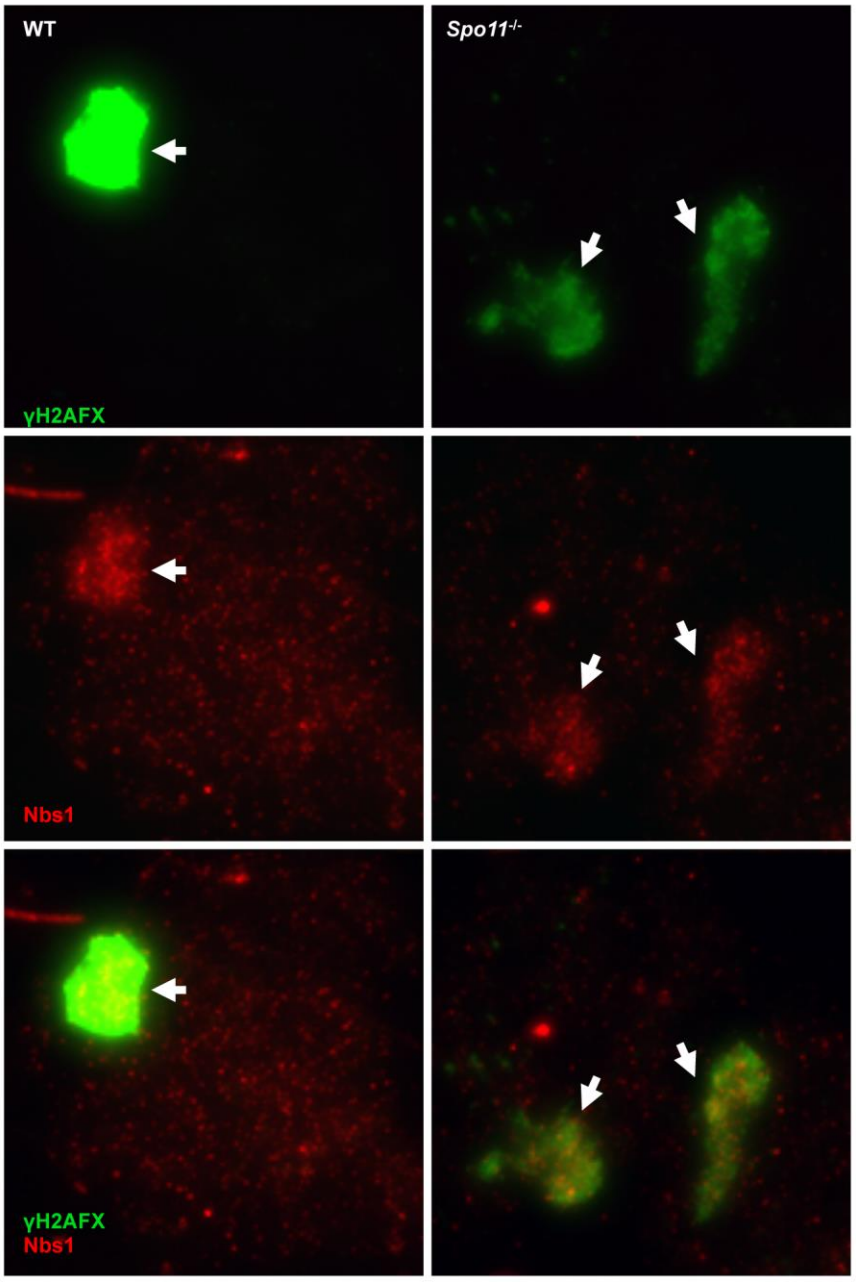

Fig. S6. Localization of Nbs1 to asynapsed chromatin in *Spo11*$^{-/-}$ spermatocytes. Indirect immunofluorescence against Nbs1 in *Spo11*$^{-/-}$ spermatocytes. Just as in WT spermatocytes, Nbs1 colocalized with γH2AFX-positive domains (white arrows) in the absence of SPO11.

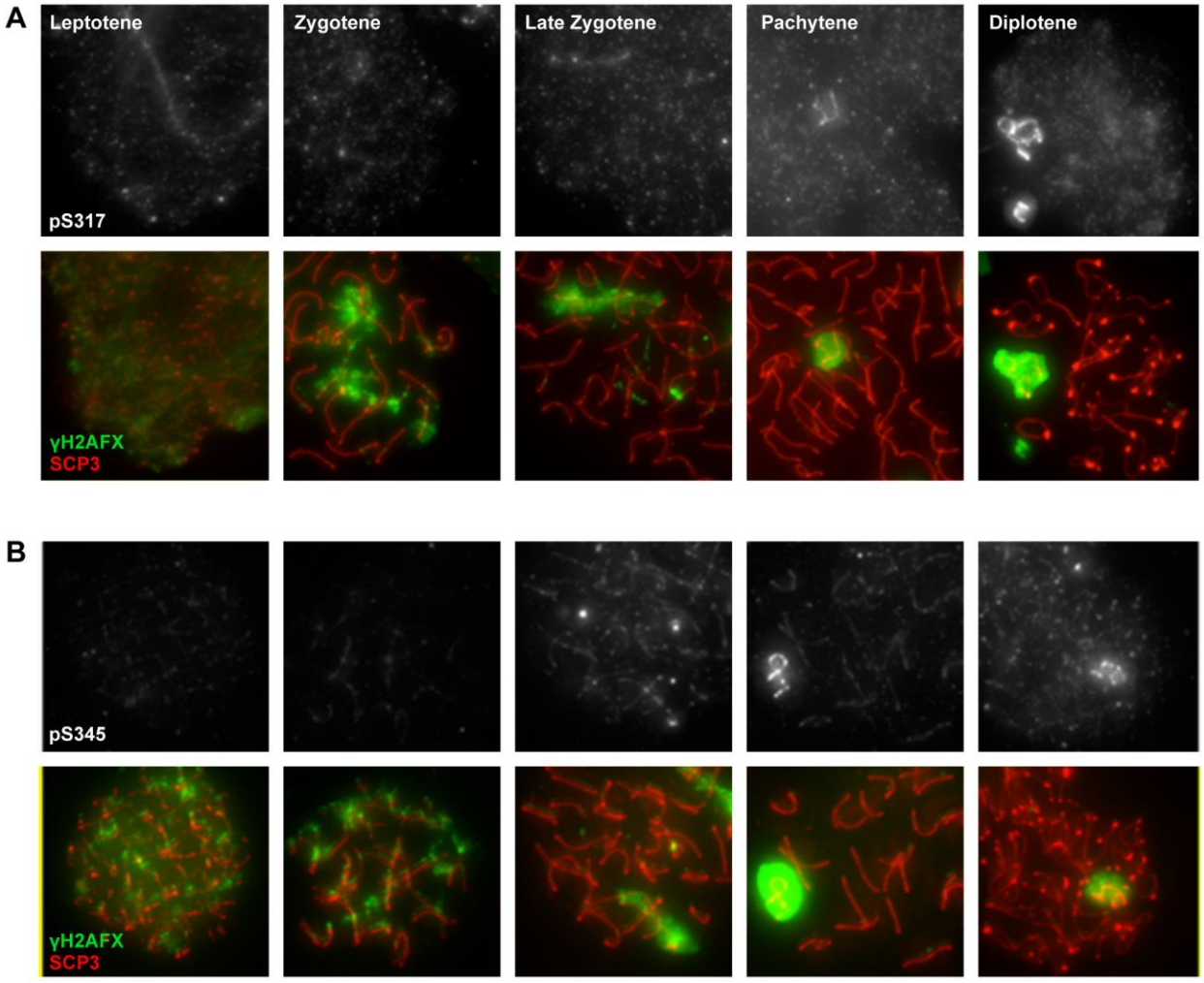

Fig. S7. Distribution of CHK1 phosphoforms in primary spermatocytes. Distribution of pCHK1 (S317) (**A**) and pCHK1 (S345) (**B**) at stages of the first meiotic prophase.

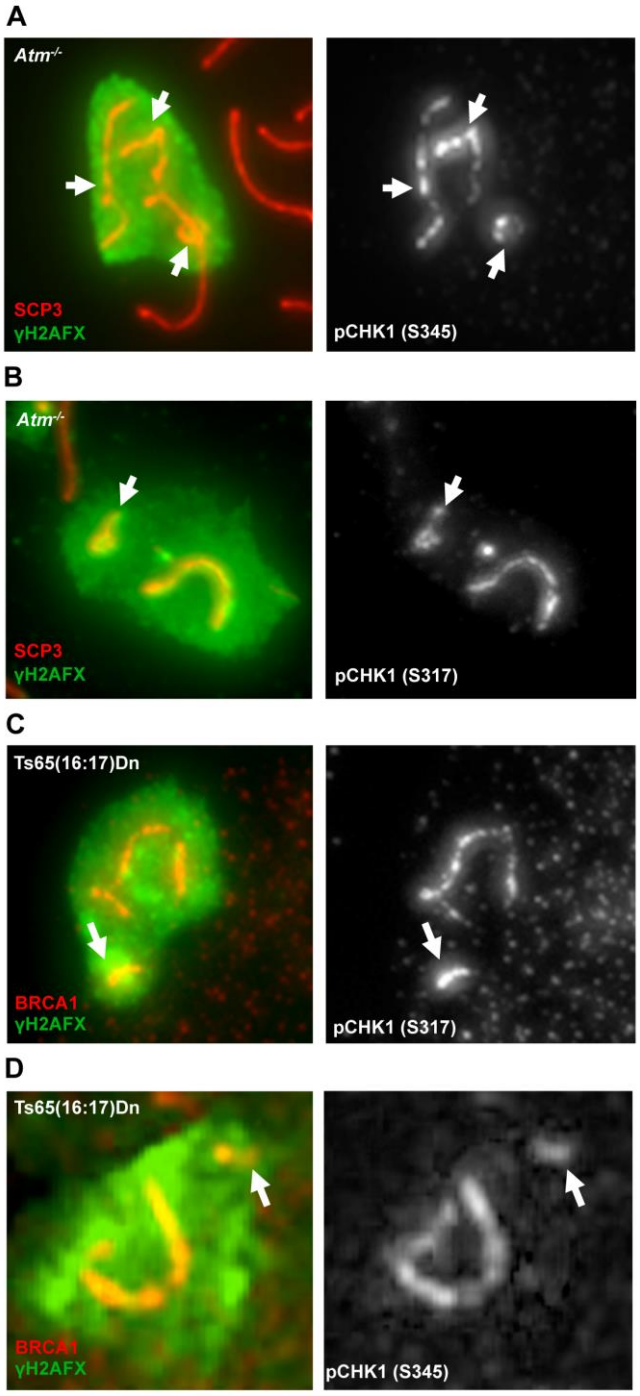

Fig. S8. Localization of CHK1 phosphoforms in *Atm*$^{-/-}$spermatocytes. Asynapsed chromosomes in *Atm*$^{-/-}$ spermatocytes are associated with pCHK1 (S317) (**A**) and pCHK1 (S345) (**B**). Similarly, both phosphorylated forms of CHK1, S317 (**C**), and S345 (**D**), are enriched on asynapsed autosomes (white arrow) in Ts65(16:17)Dn spermatocytes**.**